

# Experimental Studies on Heat Transfer in the Annuli with Corrugated Inner Tubes

Soo Whan Ahn\*

*School of Mechanical and Aerospace Engineering, Gyeongsang National University,  
Institute of Marine Industry, 445 Inpyong-dong, Tongyong, Gyongnam 650-160, Korea*

Experimental heat transfer data for single-phase water flow in the annuli with corrugated inner tubes are presented. In the annuli with parallel flow, ten different annular arrangements are considered. For water flow rate in  $1,700 < Re < 13,000$  regime, data for Nusselt numbers are presented. The results show significant effects of both the pitch to trough height ratio ( $P/e$ ) and the radius ratio ( $r^*$ ). As  $P/e$  becomes closer to 8 in the range below the radius ratio ( $r^*$ ) of 0.5, Nusselt numbers increase. However, Nusselt numbers decrease in the range above the radius ratio ( $r^*$ ) of 0.5 because flow reattachment position becomes farther in the narrower clearance.

**Key Words:** Heat Transfer Coefficient, Corrugated Annular Tube, Parallel Flow, Turbulent Flow, LMTD (Log-Mean Temperature Difference)

## Nomenclature

$A$ : Heat transfer area [ $m^2$ ]	$N$ : Number of corrugation starts
$C_p$ : Specific heat [ $kJ/kg\ K$ ]	$Nu$ : Nusselt number, $h D_h/k$
$D_b$ : Bore diameter [ $m$ ]	$P$ : Corrugation pitch [ $m$ ], pressure [ $Pa$ ]
$D_e$ : Envelope diameter [ $m$ ]	$P^*$ : Nondimensional corrugation pitch $P/D_{vo}$ [ $m$ ]
$D_h$ : Annulus hydraulic diameter, $(D_{oi} - D_{vo})$ [ $m$ ]	$Pr$ : Prandtl number, $\mu C_p/k$
$D_{oi}$ : Inner diameter of the outer smooth tube [ $m$ ]	$Q$ : Heat duty [ $W$ ]
$D_{vi}$ : Volume-based corrugated tube inner di- ameter [ $m$ ]	$R$ : Heat transfer resistance [ $K/W$ ]
$D_{vo}$ : Volume-based corrugated tube outer di- ameter [ $m$ ]	$Re$ : Reynolds number, $D_h V/\nu$
$e$ : Corrugation depth, $(D_e - D_b)/2$ [ $m$ ]	$r^*$ : Annulus radius ratio, $D_{vo}/D_{oi}$
$e^*$ : Nondimensional corrugation depth, $e/D_{vo}$ [ $m$ ]	$T$ : Temperature [ $K$ ]
$f$ : Friction factor, $2\Delta P D_h/\rho V^2 L$	$U$ : Overall heat transfer coefficient [ $W/m^2\ K$ ]
$h$ : Heat transfer coefficient [ $W/m^2\ K$ ]	$V$ : Flow velocity [ $m/s$ ]
$k$ : Thermal conductivity [ $W/m\ K$ ]	$Vol$ : Volume [ $m^3$ ]
$L$ : Tube length [ $m$ ]	$\theta$ : Corrugation helix angle, $\tan^{-1}(\pi D_{vo}/NP)$ [ $^\circ$ ]
	$\theta^*$ : Nondimensional corrugation helix angle, $\theta/90$

## Subscripts

$a$ : Annulus
$as$ : Smooth annulus
$i$ : Inner tube, inlet
$ci$ : Inlet at cold side
$co$ : Outlet at cold side
$hi$ : Inlet at the hot side

\* E-mail : swahn@gacchuk.gsnu.ac.kr

TEL : +82-55-640-3125; FAX : +82-55-640-3128

School of Mechanical and Aerospace Engineering,  
Gyeongsang National University, Institute of Marine  
Industry, 445 Inpyong-dong, Tongyong, Gyongnam 650  
-160, Korea. (Manuscript Received February 10, 2001;

Revised May 22, 2002)

$h_o$  : Outlet at the hot side  
 $s$  : Smooth  
 $t$  : Tube  
 $tot$  : Total  
 $w$  : Wall  
 $r$  : Corrugated

## 1. Introduction

The convective heat transfer coefficients may be increased by artificially roughened surfaces, inlet vortex generators, vibration of the surface, application of electrostatic fields, and modification of the duct cross section and surface. Many of these techniques increase the heat transfer coefficient through a change in flow patterns. In the recent past, some attention has been given to heat transfer augmentation by means of spiral flutes, grooves, and ridges on heat exchanger tubes (Marto et al., 1979). The spirally fluted or corrugated tube is believed to enhance the convective heat transfer by introducing swirl into the bulk flow and/or periodic disruption of the boundary layer at the tube surface due to repeated changes in the geometry. Several geometric parameters such as the inner diameter, envelope diameter, ridge, pitch, shape, and the number of starts, must be specified to define a corrugated or fluted enhanced geometry completely. These dimensions are shown in Fig. 1. A change in any of these dimensions affects the flow and heat transfer characteristics of the tube. A survey of heat transfer and friction factor studies for spirally fluted tubing was also conducted by Bergles (1980). For laminar internal heat transfer in heating, 200 percent increases in the heat transfer coefficient and friction factor were reported. For turbulent internal flow, several studies were quoted with improvements of up to 400 percent above the plain tube heat transfer coefficients, but the pressure drop was as much as 10 times higher than for plain tubes. Heat transfer and pressure drop for tubes with single- and multiple- helix internal ridging were investigated by Withers (1980a, b). An empirical correlation for friction factor in terms of the Reynolds number,  $Re$  and a set of adjustable constants was proposed. Nakayama

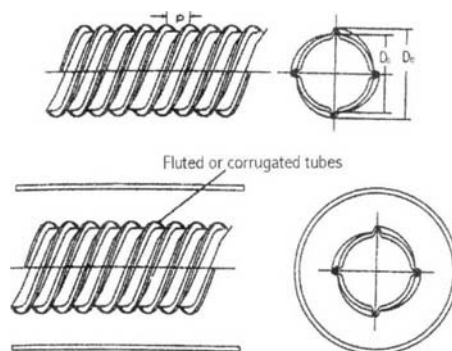


Fig. 1 Details of test section

et al. (1983) performed an experimental investigation of heat transfer enhancement for water flowing through spirally ribbed tubes in a turbulent regime. They postulated that at low helix angles, the flow near the wall follows the rib profiles, while at high helix angles, it crosses the ribs. At intermediate angles, the flow changes from swirl-dominant flow to cross-over flow. Garimella and Christensen (1995a, b) and Garimella (1990) also addressed the hydrodynamic and heat transfer aspects of the annuli with spirally fluted inner tubes in counterflow. Flow mechanisms and pressure drop measurements were used to propose the friction factor correlations. These fluted-annulus friction factor correlations can be used to develop the Nusselt number correlations in conjunction with heat transfer data. While some research has been done by previous investigators on the spirally fluted enhanced geometries, there are deficiencies in understanding of heat transfer at spirally corrugated geometries. The objective of the present study is to experimentally investigate the heat transfer characteristics of annuli formed by placing a spirally corrugated tube inside a smooth outer tube in parallel flow.

## 2. Experimental Apparatus and Data Reduction

Six spirally corrugated tubes, one fluted tube, and three smooth tubes for benchmarking purpose, selected to achieve an adequate variation in all the relevant geometric variables, were used for

**Table 1** Test matrix for temperature measurements

Annulus	Inner tube											Outer tube
	$D_b$ [mm]	$D_e$ [mm]	$D_s$ [mm]	$D_{vi}$ [mm]	$D_{vo}$ [mm]	$P$ [mm]	$N$	$r^*$	$e^*$	$P^*$	$\theta^*$	$D_o$ [mm]
T <sub>11</sub>	7.9	9.5	9.5	7.68	9.28	2	1	0.368	0.022	0.22	0.96	25.2
T <sub>12</sub>	7.9	9.5	9.5	7.52	9.12	5	1	0.362	0.044	0.55	0.89	25.2
T <sub>21</sub>	11.0	12.5	12.5	10.79	12.39	6	1	0.492	0.048	0.48	0.92	25.2
T <sub>22</sub>	10.0	12.5	12.5	10.93	12.53	10	1	0.497	0.056	0.80	0.84	25.2
ST <sub>21</sub>	11.6	12.8	12.5	10.71	12.31	10	3	0.488	0.13	0.81	0.68	25.2
T <sub>31</sub>	14.2	15.8	15.8	13.88	15.48	7	1	0.614	0.045	0.45	0.91	25.2
T <sub>32</sub>	14.2	15.8	15.8	13.97	15.57	10	1	0.618	0.045	0.64	0.89	25.2
S <sub>01</sub>	7.9	9.5	9.5	7.9	9.5			0.377				25.2
S <sub>02</sub>	11.0	12.5	12.5	10.9	12.5			0.496				25.2
S <sub>03</sub>	14.2	15.8	15.8	14.2	15.8			0.627				25.2

- $D_b$  : Bore diameter
- $D_s$  : Original smooth tube diameter
- $D_{vo}$  : Volume-based grooved tube outer diameter
- $N$  : Number of flute or corrugation starts
- $S$  : Smooth tube
- $T$  : Spirally corrugated tube
- $D_e$  : Envelope diameter
- $D_{vi}$  : Volume-based grooved tube inner diameter
- $P$  : Flute or corrugation pitch
- $D_{oi}$  : Inner diameter of outer smooth tube
- $ST_{21}$  : Spirally fluted tube

the heat transfer test. Each tube was placed in a smooth outer tube, which enabled the testing of annuli with different radius ratio shown in Fig. 1. A matrix of all the annuli for which heat transfer tests were conducted is presented in Table 1. A schematic of the flow loop and test sections is presented in Fig. 2. City water was supplied to a settling tank equipped with an overflow line. In this tank, any dissolved air escaped to the atmosphere. The overflow line ensured a constant pressure head from the inlet to the test section. To achieve the objective of this study, a test rig that allowed testing over a wide range of flow rates was required. It is essential that the temperature changes in the individual fluid streams, and the approach temperature differences used for calculation of *LMTDs*, are large enough to minimize the errors due to measurement inaccuracies. Electric heating from the tube side or the tube wall itself was deemed impractical because of the convoluted corrugated tube geometry. Steam condensation on the tube side could not be used because for laminar flow at the annuli side, the low flow rate caused the cold fluid to approach the hot side temperature within a very short distance. Therefore, a substantial part of the heat exchanger does not contribute to heat transfer but is erroneously

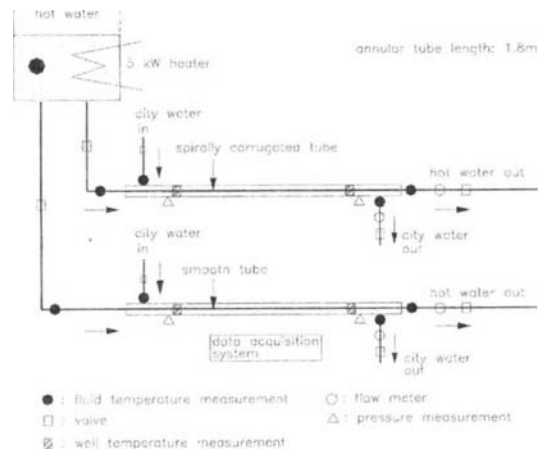


**Fig. 2** Schematic diagram of experimental setup

included in the heat transfer area calculations. Near the outlet of annulus side, the water could start boiling. Thus the present method using the single phase fluid streams in both tubes was suitable. Laminar and turbulent heat transfer tests with reasonable temperature changes in the respective streams, as well as between the hot and cold side, can be performed by using single-phase water on both sides of the heat exchanger. An appropriately controlled tube-side inlet temperature and mass flow rate would provide a high

enough ratio of  $h_t/h_a$  without causing an excessive temperature rise in the annuli fluid. As the annulus-side flow rate is increased to achieve the turbulent  $Re$  values, the tube-side flow rate can also be increased to maintain high values of tube-side heat transfer coefficient ( $h_t$ ) / annulus-side heat transfer coefficient ( $h_a$ ). Considering these factors, this method is chosen for conducting the heat transfer tests. This method does, however, require a means of calculating  $h_t$  with an accuracy that depends on the specific value of  $h_t/h_a$  in question. A cold water supply line and a supply of hot water were used for the tests. The city water line was split into two different streams. One stream was used as the cold water inlet to the annulus side of the test section. The other stream was heated by an electrical heater (Cartridge type, 5 kW) to provide the desired flow rate of hot water at the required inlet temperature. The hot water passed through the heat exchanger and exited to the drain. Cold water from the outlet of test section was supplied to the combination of control valves, from which it flowed through a flow meter of cumulative type.

The measured flow rate was used to calculate the heat duty in the heat exchanger and the annulus  $Re$ . The cold water flowed through the parallel flow heat-exchanger test section and exited to the drain. The test section consisted of a 1.8-m-long heat exchanger, insulated on the outside, formed by placing the various tubes inside a smooth outer tube. We measured the inlet and outlet temperatures of the tube side and shell side for overall energy balance by a data acquisition system. Thermocouple ports (for K-type thermocouples) were also provided at 30 cm and 150 cm from the ends of the inner tube. Numerical values and graphs of temperatures as a function of time were displayed and recorded on a computer to allow confirmation of the steady state. During the tests, the ratio of tube-side to annulus-side flow was kept at about five whenever feasible. Because the annulus-side flow area was typically larger than that of the tube side, this ratio of mass-flow rates resulted in higher ratio of heat transfer resistances. This control strategy helped in minimizing the sensitivity of the deduced annulus-side

heat transfer coefficient ( $h_a$ ) values to errors in the tube-side correlations. The Reynolds number was calculated from the measured flow rate based on the hydraulic diameter,  $D_h$ . The flow velocity was calculated by using the cross-sectional flow area. It should be noted that the corrugated tube did not have a circular cross section; therefore, a diameter that represented the average cross-sectional area of the corrugated tubes was calculated from the volume of water required to fill a given length of tubing as follows:

$$D_{vi} = \sqrt{\frac{4 Vol}{\pi L}} \tag{1}$$

The volumetric outside diameter,  $D_{vo}$ , which is the quantity of interest for the annulus side, is calculated by adding twice the tube thickness to  $D_{vi}$ . The heat duties of the two fluid streams were calculated from the flow rates and the temperature changes in the respective streams from the inlet to the outlet. The discrepancy between  $Q_a$  and  $Q_t$  was less than 6% even at the worst situation. The overall heat transfer coefficient  $UA_{tot}$  was calculated as follows:

$$UA_{tot} = \frac{Q_{tot}}{LMTD_{tot}} \tag{2}$$

$$LMTD = \frac{(T_{ho} - T_{co}) - (T_{hi} - T_{ci})}{\ln[(T_{ho} - T_{co}) / (T_{hi} - T_{ci})]} \tag{3}$$

where  $LMTD$  means the log-mean temperature difference in parallel flow. The subscripts  $tot$  represents the total heat exchanger, in addition,  $h_i$  and  $h_o$  refer to the inlet and outlet at the hot fluids and  $c_i$  and  $c_o$  refer to the inlet and outlet at the cold fluids, respectively. Heat duties,  $LMTDs$ , and  $UAs$  are also calculated by using the equations shown above for this fully developed heat exchangers for each data point for all the annuli. The overall  $U$  value ( $UA/\pi D_{vo}L$ ) is comprised of the conductance of the tube side, the tube wall, and the annulus side. Tube side flow is always maintained in the turbulent regime, and the corresponding tube-side  $Nu$  for  $Re > 700$  is given by Ravigururajan and Bergles (1985) as follows:

$$\frac{Nu_r}{Nu_s} = (1 + [2.64 Re^{0.036} e^{*0.212} Pr^{*-0.21} \times (\beta^*)^{0.29} Pr^{-0.024}]^7)^{1/7} \quad (4)$$

In the correlation heat transfer data for smooth tubes, several investigators have used an equation that incorporated the corresponding friction factor. One such example is the Petukhov and Popov correlation (1963). Because the Nusselt numbers for fluted annuli showed a departure from laminar behaviour at Reynolds numbers as low as 700, it was assumed that such an approach would be applicable for  $700 < Re < 40,000$  with a modification as follows (Garimella and Christensen, 1995);

$$Nu_s = \frac{(f_s/8) Re Pr}{1 + 12.7 \sqrt{f_s/8} (Pr^{2/3} - 1)} \quad (5)$$

where  $f_s$  is the smooth-tube friction factor (Petukhov, 1970):

$$f_s = 4[1.58 \ln(Re) - 3.28]^{-2} \quad (6)$$

These equations were applied to calculate the tube-side heat transfer coefficient based on the corrugated-tube outer volumetric diameter as follows:

$$h_t = \frac{Nu_r \cdot k}{D_{vi}} (D_{vi}/D_{vo}) \quad (7)$$

The tube wall presents the following resistance to heat transfer:

$$R_w = \frac{D_{vo}}{2k_w} \ln(D_{vo}/D_{vi}) \quad (8)$$

From the above equations, the heat transfer coefficient of the annulus ( $h_a$ ) was calculated from the following equation;

$$U = \frac{1}{1/h_t + R_w + 1/h_a} \quad (9)$$

and Nusselt number in the annulus is given by

$$Nu_a = h_a D_h / k \quad (10)$$

Uncertainties in the reported values of  $Nu$  were evaluated by using the compounding-of-errors technique (Kline and McClintock, 1953). The uncertainty in the calculation of  $Nu$  consists of three major components, uncertainty in  $U$ , and uncertainty in deriving  $Nu$  from  $U$ , and the  $h_t$  prediction. From the correlation by Ravigururajan and Bergles (1985), the uncertainty in the

tube-side resistance may be conservatively estimated to be  $\pm 25\%$ . By combining this with the uncertainty in  $U$  calculated above, the uncertainty of  $Nu$  is  $\pm 16\%$ .

### 3. Results and Discussion

Three smooth-tube annuli were tested for benchmarking purpose as shown in Fig. 3. The Nusselt numbers were higher with smaller radius ratio ( $r^*$ ). This phenomena might be attributed to the definition of Reynolds number. The data correlated by Eq. (11) and Garimella and Christensen's experimental results (1995) for smooth-tube annuli were included for a comparison. The graph shows good correspondence between the present results and the literature values.

These researchers presented turbulent heat transfer data for  $Re < 5,000$ . The data from Kays and Leung (1963) were correlated by Garimella and Christensen (1995) and the resulting equation was assumed also to apply for  $Re$  values between 3,000 and 5,000, with recognition that the potential for error for  $Re < 5,000$  would be high. The correlation was as follows;

$$Nu_{as} = 0.22 Pr^{0.5} Re_{as}^{0.8} \quad (11)$$

where the subscript *as* refers to a smooth annulus. Kays and Crawford (1993) reported that Nusselt number was 6.18 in the fully developed laminar annular tube with radius ratio ( $r^*$ ) of 0.5. However, Nusselt number in the present work was much higher than 6.18 for  $Re < 2,300$ . Thus, it is needed to investigate the transition region between laminar and turbulent flow. Garimella (1990) and Garimella and Christensen (1993) showed from the flow visualization tests of flute-tube annuli that the fluid did not flow exclusively in trough and crest zones near an enhanced-tube wall and in a purely axial flow away from the wall, but in a spiral pattern, alternatively crossing over the trough and crest. Their tests also confirmed that a Reynolds number of 800 adequately delineated laminar and turbulent flow. Therefore, it seemed that the present work covering annuli with corrugated core tubes would have a similar flow pattern.

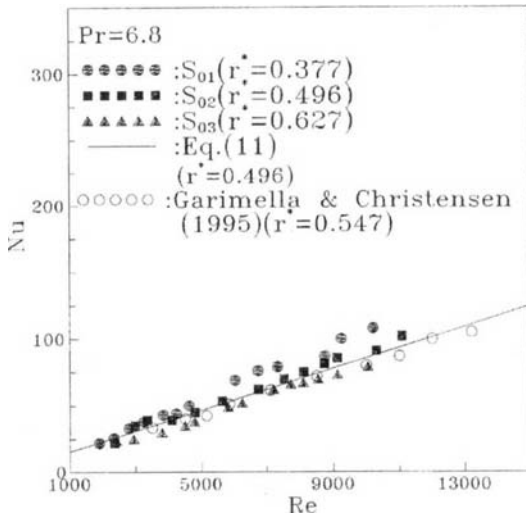


Fig. 3 Nusselt numbers for smooth annuli

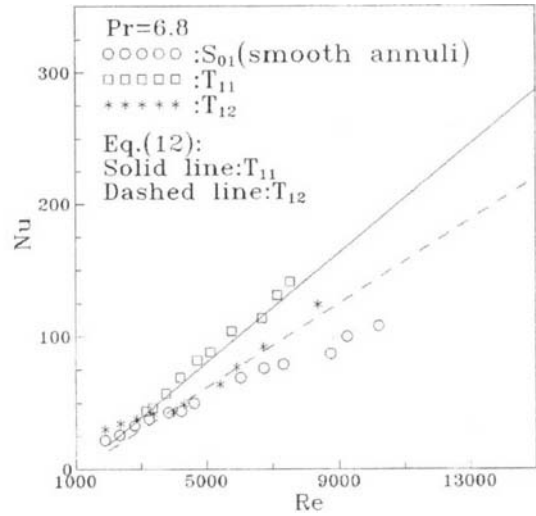


Fig. 4 Nusselt numbers for corrugated annuli,  $T_{11}$  and  $T_{12}$

Figure 4 shows the variations of Nusselt numbers in the annuli having the corrugated core tubes,  $T_{11}$  and  $T_{12}$ . The Nusselt numbers in  $T_{11}$  of pitch to trough height ratio ( $P/e$ ) = 10 are somewhat higher than in  $T_{12}$  of 12.5. This phenomena have similar tendencies to Lawn's results (1974) that Nusselt numbers become highest around  $P/e=8$  and lower at the situation farther away from  $P/e=8$ . This feature is in a line with Wilkie (1966) and Ahn et al. (1994) showing that the highest heat transfer occurs when the roughness pitch and flow reattachment are equal. We derived the empirical correlations for the annuli having the corrugated core tubes as follows ;

$$r^* < 0.5 : Nu_a = (0.115Pr + 0.1987) (-4.94652 \times 10^{-7} Re^2 + 0.026896 Re - 36.25) \times [0.0211(P/e)^2 - 0.528(P/e) + 3.742] r^{*-0.55} \quad (12)$$

$$r^* > 0.5 : Nu_a = (0.115Pr + 0.1987) (7.268 \times 10^{-8} Re^2 + 0.01054 Re + 15.3) \times [0.0281(P/e) + 0.499] r^{*-0.55} \quad (13)$$

The solid and dashed lines indicate the data obtained from the empirical correlations for  $T_{11}$  and  $T_{12}$ . The empirical correlations provide a fairly good representation of variations of experimental data. The Nusselt numbers in the annuli with corrugated core tubes of  $T_{21}$  and  $T_{22}$ , and with spirally fluted core tube of  $ST_{21}$  are shown

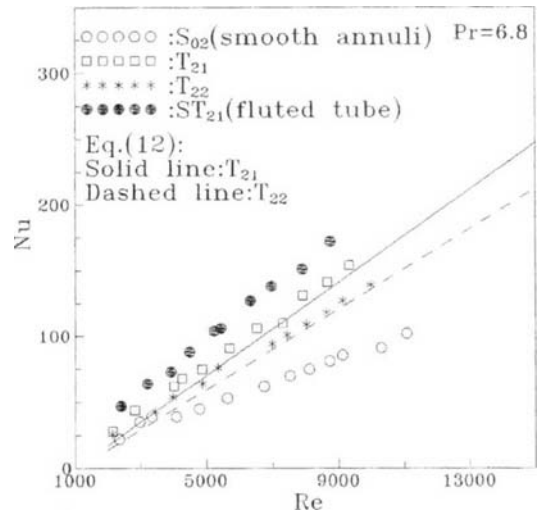


Fig. 5 Nusselt numbers for corrugated and fluted annuli,  $T_{21}$ ,  $T_{22}$  and  $ST_{21}$

in Fig. 5. The values in  $ST_{21}$  are much higher than in  $T_{21}$  and  $T_{22}$ . This effect might be caused by the fact that the trough, corresponding to the roughness height, in the spirally fluted tube has higher. Nusselt numbers for  $T_{31}$  and  $T_{32}$  are indicated in Fig. 6. Careful inspection of this figure further shows that, being different from Figs. 4 and 5, the heat transfer in  $T_{32}$  having pitch to trough height ratio ( $P/e$ ) of 14.2 is higher than in  $T_{31}$  having  $P/e$  of 10. This feature is attributed

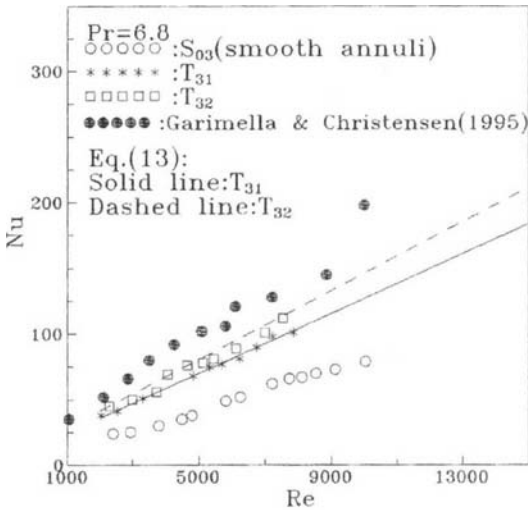


Fig. 6 Nusselt numbers for corrugated annuli,  $T_{31}$  and  $T_{32}$

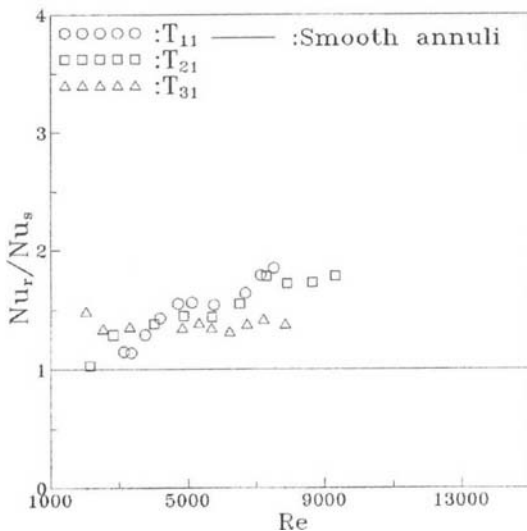


Fig. 7 Nusselt numbers normalized by smooth annuli

to the fact that the flow reattachment occurs at the position farther away from the vicinity of the ridge in the annuli with higher radius ratio. For a comparison, Garimella and Christensen's data (1995), covering the annuli with spirally fluted core tube, are involved. It is shown that the same features as in Fig. 5 are retained. Nusselt numbers non-dimensionalized by a smooth channel are represented in Fig. 7. The data for the smooth

annuli using Eq. (11) are indicated as a reference. The effects of Nusselt numbers on the radius ratio were not simple for the flow in the annuli with square-ribbed surface roughness elements on the outer tubes only (Ahn et al., 1994). The normalized Nusselt numbers increased with the radius ratio. However, in the present study, normalized Nusselt numbers usually increased with decreasing the radius ratio. The reason for discrepancy between the two cases is not known for the moment because lack of flow data over the annuli with rough surfaces makes it difficult to speculate on probable cause.

#### 4. Conclusion

The present work shows the experimental heat transfer data for single-phase water flow in the annuli with corrugated inner tubes. In the annuli with parallel flow, ten different annular arrangements for water flow rate in the  $1,700 < Re < 13,000$  regime are considered. The following conclusions can be drawn :

(1) In the range below the radius ratio ( $r^*$ ) of 0.5, the Nusselt numbers in  $T_{11}$  of pitch to trough height ratio ( $P/e$ ) = 10 are somewhat higher than in  $T_{12}$  of 12.5. It is because the radial directional fluctuating components are strongly produced in the equality between the roughness pitch and flow reattachment distance.

(2) However, the heat transfer in  $T_{32}$  having pitch to trough height ratio ( $P/e$ ) of 14.2 is higher than in  $T_{31}$  having  $P/e$  of 10 in the range above the radius ratio ( $r^*$ ) of 0.5 because the flow reattachment occurs at the position farther away the vicinity of the ridge in the annuli with higher radius ratio.

(3) The Nusselt numbers in the annuli with spirally fluted core tube of  $ST_{21}$  are much higher than in the annuli with corrugated core tubes of  $T_{21}$  and  $T_{22}$  because the trough, corresponding to the roughness height, is higher in the spirally fluted tube.

#### References

Ahn, S. W., Kim, K. C. and Lee, Y. P., 1994,

"Fully Developed Turbulent Flow and Heat Transfer in Concentric Annuli With Square-Ribbed Roughness," *Trans. KSME*, Vol. 18, No. 4, pp. 1072~1088.

Bergles, A. E., 1980, *Heat Transfer Characteristics of Turbotec Tubing*, Heat Transfer Laboratory Report HTL-24 ISU-ER1-Ames-81018, Iowa State University.

Garimella, S., 1990, *Experimental Investigation of Heat Transfer and Pressure Drop Characteristics of Annuli With Spirally Fluted Inner Tubes*, Ph. D. Dissertation, The Ohio State University.

Garimella, S. and Christensen, R. N., 1993, "Experimental Investigation of Fluid Flow Mechanisms in Annuli with Spirally Fluted Inner Tubes," *ASHRAE Trans.* Vol. 99, Part 1, pp. 1205~1216.

Garimella, S. and Christensen, R. N., 1995a, "Heat Transfer and Pressure Drop Characteristics of Spirally Fluted Annuli: Part I- Hydrodynamics," *ASME Journal of Heat Transfer*, Vol. 117, No. 54, pp. 54~60.

Garimella, S. and Christensen, R. N., 1995b, "Heat Transfer and Pressure Drop Characteristics of Spirally Fluted Annuli: Part II- Heat Transfer," *ASME Journal of Heat Transfer*, Vol. 117, No. 54, pp. 61~68.

Kays, W. M. and Crawford, M. E., 1993, *Convective Heat and Mass Transfer*, McGraw-Hill Co., pp. 138~152.

Kays, W. M. and Leung, E. Y., 1963, "Heat Transfer in Annular Passages: Hydrodynamically Developed Flow with Arbitrarily Prescribed Heat Flux," *Int. J. Heat Mass Transfer*, Vol. 6, pp. 537~557.

Kline, S. J. and McClintock, F. A., 1953, "Describing Uncertainties on Single Sample Experiments," *Mechanical Engineering*, Vol. 57, pp. 3~8.

Lawn, C. J., 1974, "The Use of an Eddy Viscosity Model to Predict the Heat Transfer and Pressure Drop Performance of Roughened Surfaces," *Int. J. Heat Mass Transfer*, Vol. 17,

pp. 421~428.

Marto, P. J., Reilly, R. J. and Fenner, J. H., 1979, "An Experimental Comparison of Enhanced Heat Transfer Condenser Tubing in: Advance in Heat Transfer," ASME, New York, pp. 1~9.

Nakayama, W., Takahashi, K., and Daikoku, T., 1983, "Spiral Ribbing to Enhance Single Phase Heat Transfer Inside Tubes," *ASME-JSME Thermal Engineering Joint Conference Proceedings*, Honolulu, HI, Vol. 1, pp. 365~372.

Petukhov, B. S., 1970, *Heat Transfer and Friction in Turbulent Pipe Flow Variable Physical Properties*, in: *Advance in Heat Transfer*, T. F. Irvine and J. P. Hartnett, Vol. 6, Academic Press, New York, pp. 503~564.

Petukhov, B. S. and Popov, V. N., 1963, "Theoretical Calculation of Heat Exchange and Frictional Resistance in Turbulent Flow in Tubes of an Incompressible Fluid With Variable Physical Properties," *High Temperature*, Vol. 1, pp. 69~83.

Ravigururajan, T. S. and Bergles, A. E., 1985, "General Correlation for Pressure Drop and Heat Transfer for Single Phase Turbulent Flow in Internally Ribbed Tubes, in: Augmentation of Heat Transfer in Energy System," *ASME-HTD*-Vol. 52, pp. 9~20.

Wilkie, D., 1966, "Forced Convection Heat Transfer from Surface Roughened by Transverse Ribs," *3rd International Heat Transfer Conference*, Chicago, Illinois, Vol. 1, p. 19.

Withers, J. G., 1980a, "Tube-Side Heat Transfer and Pressure Drop for Tubes Having Helical Internal Ridging With Turbulent/Transitional Flow of Single Phase Fluid, Part 1. Single-Helix Ridging," *Heat Transfer Engineering*, Vol. 2, No. 1, pp. 48~58.

Withers, J. G., 1980b, "Tube-Side Heat Transfer and Pressure Drop for Tubes Having Helical Internal Ridging with Turbulent/Transitional Flow of Single Phase Fluid, Part 2. Multiple Helix Ridging," *Heat Transfer Engineering*, Vol. 2, No. 2, pp. 43~50.